

# Boronic Acid: A Bio-Inspired Strategy To Increase the Sensitivity and Selectivity of Fluorescent NADH Probe

Lu Wang,<sup>†</sup> Jingye Zhang,<sup>‡</sup> Beomsue Kim,<sup>§</sup> Juanjuan Peng,<sup>§</sup> Stuart N. Berry,<sup>§</sup> Yong Ni,<sup>§</sup> Dongdong Su,<sup>§</sup> Jungyeol Lee,<sup>†</sup> Lin Yuan,<sup>||</sup> and Young-Tae Chang<sup>\*,†,§</sup>

<sup>†</sup>Department of Chemistry and Medicinal Chemistry Program, National University of Singapore, Singapore 117543

<sup>‡</sup>Key Laboratory of Smart Drug Delivery, Ministry of Education, School of Pharmacy, Fudan University, Shanghai 201203, P. R. China

<sup>§</sup>Laboratory of Bioimaging Probe Development, Singapore Bioimaging Consortium, Singapore 117543

<sup>||</sup>State Key Laboratory of Chemo/Biosensing and Chemometrics, College of Chemistry and Chemical Engineering, Hunan University, Changsha 410082, P. R. China

## Supporting Information

**ABSTRACT:** Fluorescent probes have emerged as an essential tool in the molecular recognition events in biological systems; however, due to the complex structures of certain biomolecules, it remains a challenge to design small-molecule fluorescent probes with high sensitivity and selectivity. Inspired by the enzyme-catalyzed reaction between biomolecule and probe, we present a novel combination-reaction two-step sensing strategy to improve sensitivity and selectivity. Based on this strategy, we successfully prepared a turn-on fluorescent reduced nicotinamide adenine dinucleotide (NADH) probe, in which boronic acid was introduced to bind with NADH and subsequently accelerate the sensing process. This probe shows remarkably improved sensitivity (detection limit: 0.084  $\mu\text{M}$ ) and selectivity to NADH in the absence of any enzymes. In order to improve the practicality, the boronic acid was further modified to change the measurement conditions from alkaline (pH 9.5) to physiological environment (pH 7.4). Utilizing these probes, we not only accurately quantified the NADH weight in a health care product but also evaluated intracellular NADH levels in live cell imaging. Thus, these bio-inspired fluorescent probes offer excellent tools for elucidating the roles of NADH in biological systems as well as a practical strategy to develop future sensitive and selective probes for complicated biomolecules.

Optical imaging as a noninvasive imaging technique has been widely used in exploration of biological processes, disease diagnosis, and treatment.<sup>1–3</sup> Fluorescent probes sensing the target biomolecules or biological microenvironment are an indispensable part in the imaging process.<sup>4–9</sup> Ideal fluorescent probes should contain several basic requirements, such as suitable sensitivity, high selectivity, good stability, short response time, and dynamic changes of fluorescent properties.<sup>10</sup> Among the various characters of the fluorescent probes, sensitivity and selectivity are particularly important to detect specific biomolecules, especially in complicated biological systems, such as live cells.<sup>11</sup> However, due to the complex structures of certain

biomolecules, it remains a challenge to reasonably design fluorescent probe with satisfied sensitivity and selectivity simultaneously.

Among the complex biomolecules, the representative reduced nicotinamide adenine dinucleotide (NADH) consists of one adenine, one nicotinamide, two ribose rings, and a pair of bridging phosphate groups (Figure S1). The complicated structure makes it difficult to design ideal probes to detect in biological systems. However, NADH and its oxidized form, NAD<sup>+</sup>, are the most indispensable coenzymes found in all living cells and are required in multiple biological processes.<sup>12–17</sup> Thus, it is of considerable interest to prepare probes for monitoring NADH levels in biological systems.

Recently, several offline methods, including a conventional enzymatic cycling assay,<sup>18</sup> high-performance liquid chromatography,<sup>19</sup> and capillary electrophoresis,<sup>20</sup> have been developed to quantify NADH *in vitro*. Further, the intrinsic fluorescence of NADH has been used in the quantification and imaging of biological samples,<sup>21,22</sup> however, its short excitation/emission wavelength can be easily interfered with by other biomolecules, such as proteins. To the best of our knowledge, except macromolecular fluorescent probes based on genetically encoded proteins and nanoparticles,<sup>23–26</sup> several small-molecule fluorescent NADH probes have been reported, but only two were applied in live cell imaging.<sup>27–31</sup> The current design strategy is mainly based on the redox reaction between NADH and probe, along with alteration of the probes' fluorescence intensity or wavelength. However, due to lack of recognition groups in the above probes, the selectivity of these probes to NADH is still not sufficient. Furthermore, other deficiencies, such as turn-off fluorescent response and low sensitivity, also limited their application in cell imaging. Thus, it is urgent to prepare a fluorescent probe that selectively and sensitively detects NADH in live cells.

Since first reported in the 1960s, the enzymatic cycling assay has been used to quantify NADH concentrations *in vitro* and evaluate NADH-related enzyme activities.<sup>32</sup> As shown in Figure 1A, in the presence of enzymes, probe and NADH can be fixed

Received: June 7, 2016

Published: August 8, 2016

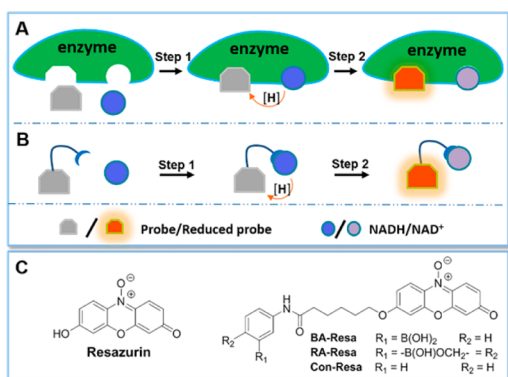


**Figure 1.** (A) Scheme of the enzyme-catalyzed NADH sensing process. (B,C) Design and structures of NADH probes.

into the binding sites of the enzyme and localized in close proximity in specific sites, which promotes hydride transfer and accelerates the redox reaction. However, the high price and strict measurement condition of this method limit the application in biosamples, especially in live cells. Inspired by the enzyme-catalyzed reaction for NADH detection and ligand-directed protein labeling,<sup>33</sup> we proposed a novel combination-reaction two-step sensing strategy to design small-molecule fluorescent probes. Specifically, a recognition group was introduced in the probe to combine with NADH, which subsequently accelerates the sensing process in the absence of any enzymes (Figure 1B). As shown in Figure S1, NADH can be divided into two parts: reaction site, nicotinamide, and recognized sites, ribose or pyrophosphate linker. In this work, resazurin was chosen as the fluorophore due to its excellent performance for evaluating reductase activity.<sup>34</sup> In the case of binding group, boronic acid was selected because it has been widely applied in the recognition of diol-containing biomolecules, such as carbohydrates<sup>35</sup> and nucleoside polyphosphates (NPPs).<sup>36</sup> It was hypothesized that the combination of boronic acid of the probe and ribose of NADH would shorten the spatial distance and facilitate hydride transfer, thereby accelerating the reduction of weakly fluorescent resazurin derivatives to strongly fluorescent products. Thus, 3-aminophenylboronic acid was connected to resazurin via an alkane linker (Figure 1C and Scheme S1). The probes were prepared and characterized by spectroscopy, <sup>1</sup>H NMR, <sup>13</sup>C NMR, and high-resolution mass spectrometry (Supporting Information).

Initially, the spectroscopic properties of BA-Resa (10 μM) responding to NADH were examined in the buffer solution (pH 9.5; DMSO/water = 1/99 v/v, 10 mM PBS) (Table S1). As displayed in Figures 2A and S2, the decreased absorption band at 535 nm and the increased band at 485 nm were observed simultaneously upon the addition of NADH (0–50 μM). At the same time, the maximum fluorescence wavelength was shifted from 620 to 575 nm in accompaniment with a 38.6-fold emission turn-on response (Figures 2B and S3). This is consistent with the reduction of the weakly fluorescent resazurin to strongly fluorescent resorufin.<sup>37</sup> Notably, the response of BA-Resa to NADH at low concentrations (0–1 μM) also showed excellent linearity with detection limit as low as 0.087 μM (Figure S4). Furthermore, in control experiments with Con-Resa and Resazurin, there were few spectral changes, thus demonstrating the remarkably enhanced sensitivity of this two-step sensing strategy (Figure S5). It was also shown that this sensing process could be achieved within 25 min (Figure S6). pH titration

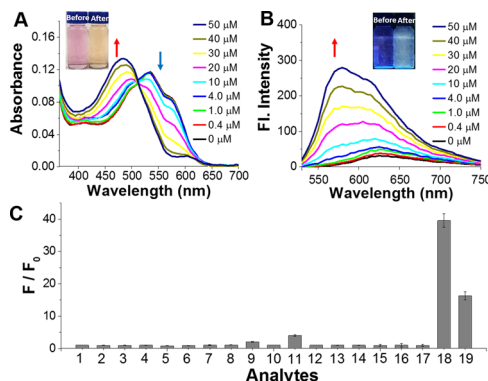


**Figure 2.** (A) UV-vis absorption and (B) fluorescence spectra of BA-Resa with titration of NADH as a function of concentration (0–50 μM). DMSO/PBS (1/99, pH 9.5). (C) Fluorescence response of BA-Resa to various biomolecules. Analytes (2–7, 1 mM; 8–19, 50 μM): (1) buffer, (2) Ca<sup>2+</sup>, (3) K<sup>+</sup>, (4) Na<sup>+</sup>, (5) Fe<sup>3+</sup>, (6) Zn<sup>2+</sup>, (7) Mg<sup>2+</sup>, (8) tyrosine, (9) cysteine, (10) methionine, (11) GSH, (12) glucose, (13) ribose, (14) fructose, (15) ATP, (16) ADP, (17) NAD<sup>+</sup>, (18) NADH, (19) NADPH.  $F/F_0$  represents the fluorescence intensity ratio at 575 nm, and  $F_0$  is the fluorescence intensity of BA-Resa without NADH. Measurement condition: [BA-Resa] = 10 μM, 10 mM phosphate buffer saline (pH 9.5) solution,  $\lambda_{\text{ex}}$  = 480 nm, 37 °C, and incubation time: 20 min. Results are expressed as mean ± standard deviation of three independent experiments.

experiments indicated that higher pH benefits the fluorescent response of BA-Resa to NADH (Figure S7), which is probably due to the favorable combination between probe and NADH in alkaline environment.

Oxidized nicotinamide adenine dinucleotide (NAD<sup>+</sup>), the oxidized form of NADH, is a persistent source of interference in traditional NADH detection methods. However, it was shown that the fluorescence signal of BA-Resa remains silent in the presence of NAD<sup>+</sup> even at high concentration and long incubation time (Figure S8). Meanwhile, we further evaluated the selectivity of BA-Resa toward NADH by comparing with common biomolecules. As shown in Figure 2C, negligible fluorescence enhancement was observed after incubation with metal ions (2–7), amino acids (9–11), carbohydrates (12–14), and NPPs (15–16), demonstrating the potential of this NADH probe in live cell imaging. Interestingly, even though it shares the same reducing functional group with NADH, reduced nicotinamide adenine dinucleotide phosphate (NADPH, 19) generated a much lower fluorescence signal (Figures 2C and S9). This could be because the partially phosphorylated ribose in NADPH reduces the possibility of combination with boronic acid of the probe, thereby slowing the reaction rate.

To confirm the function of boronic acid in the proposed sensing process, control probe Con-Resa without boronic acid was prepared (Scheme S1). As shown in Figure S5, after incubation with NADH (0–100 μM), few spectral changes of control probe Con-Resa were observed. However, the mixture of NADH and boronic acid-containing probe BA-Resa displayed blue-shifted wavelength and increased fluorescence intensity. These spectral changes indicate the production of reduced fluorophore (BA-Resa-P), which is consistent with the calculated results (Figure S10). Meanwhile, the redox reaction in the sensing process was also demonstrated by liquid chromatography-mass spectrometry (LC-MS) (Figure S11). Therefore, a two-step sensing mechanism of the boronic acid-containing probe responding to NADH was proposed and

displayed in Figure 3. First, the boronic acid of BA-Resa and either of diols in NADH initially form the boronic ester of

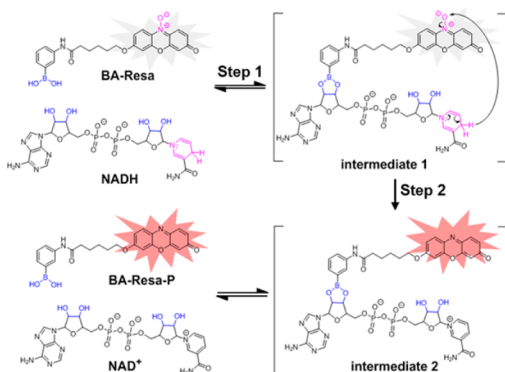


**Figure 3.** Proposed mechanism of probe BA-Resa responding toward NADH. The binding with boronic acid could be to either of two riboses in NADH (blue).

intermediate 1. Second, the shorter distance in intermediate 1 facilitates the hydride transfer from NADH to probe BA-Resa, thereby accelerating the reduction of the weakly fluorescent BA-Resa to the strongly fluorescent BA-Resa-P (more discussion in Figure S11 legend). Notably, the assumptive boronic ester-containing intermediate 1 was confirmed by MALDI-TOF mass spectrometry (Figure S12).

Even though BA-Resa was successfully applied to detect NADH in buffer solution, the alkaline measurement conditions limit the applications in biological systems. To address this problem, the phenylboronic acid of BA-Resa was replaced by 2-(hydroxymethyl)phenylboronic acid, which forms boronic esters with diols of ribose at physiological pH (7.4).<sup>38</sup> As shown in Figures 4 and S13, in pH 7.4 buffer solution, only slightly enhanced fluorescence intensity of BA-Resa was obtained in the presence of NADH; however, probe RA-Resa emitted a remarkably increased fluorescence with detection limit as low as 0.41  $\mu\text{M}$  under the same conditions. This is mainly because 2-(hydroxymethyl)phenylboronic acid of RA-Resa is favorable for binding with NADH at pH 7.4, accelerating the redox reaction (Figure S14). The pH effect on the spectral changes of RA-Resa responding to NADH was examined and listed in Figure S15. Interestingly, in pH 7.4 buffer solution, probe RA-Resa not only showed significantly enhanced sensitivity to NADH but also displayed improved selectivity in the presence of biomolecules (Figures 4D, S16–18). With the advantages of RA-Resa demonstrated, we next tested the feasibility of RA-Resa to detect NADH produced in an enzyme system. As shown in Figure S19, increased fluorescence intensity was observed only in the presence of alcohol dehydrogenase, NAD<sup>+</sup> and ethanol, indicating the potential of RA-Resa to study the NAD<sup>+</sup>-dependent enzyme activities. In addition, NADH is contained in lots of dietary supplements, but its strong reduction ability makes it easily oxidized to NAD<sup>+</sup>. In this work, probe RA-Resa was also successfully used to accurately measure the NADH content of dietary supplement in a fluorescence assay (Figure S20).

Inspired by the excellent performance of this NADH probe *in vitro*, we evaluated the application of RA-Resa for detecting NADH in live oral squamous cell carcinoma (OSCC) cells. Initially, we performed the MTT assay by incubating with RA-Resa at different concentrations for 6 and 24 h, respectively. The results indicate the low cytotoxicity of the probe RA-Resa in live

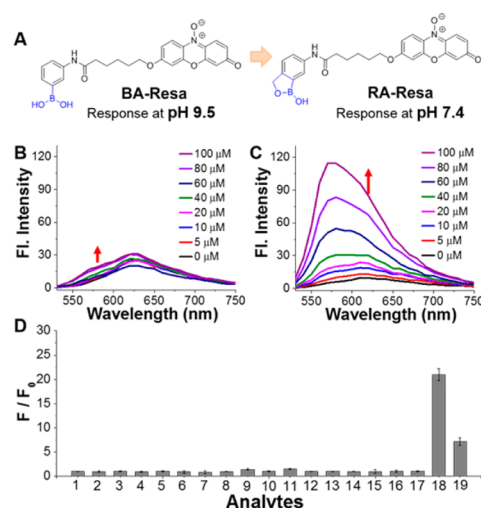


**Figure 4.** A) The structures of NADH probe BA-Resa and RA-Resa. The emission spectra of BA-Resa (B) and RA-Resa (C) responding to NADH at physiological pH (7.4). (D) Fluorescence response of RA-Resa to various biomolecules. Analytes (2–7, 1 mM; 8–19, 100  $\mu\text{M}$ ): (1) buffer, (2) K<sup>+</sup>, (3) Na<sup>+</sup>, (4) Ca<sup>2+</sup>, (5) Zn<sup>2+</sup>, (6) Fe<sup>3+</sup>, (7) Mg<sup>2+</sup>, (8) tyrosine, (9) cysteine, (10) methionine, (11) GSH, (12) glucose, (13) ribose, (14) fructose, (15) ATP, (16) ADP, (17) NAD<sup>+</sup>, (18) NADH, (19) NADPH.  $F/F_0$  represents the fluorescence intensity ratio, and  $F_0$  is the fluorescence intensity at 575 nm of RA-Resa without NADH. Measurement condition: [Probes] = 10  $\mu\text{M}$ , 10 mM phosphate buffer saline (pH 7.4) solution,  $\lambda_{\text{ex}}$  = 480 nm, 37  $^{\circ}\text{C}$ , and incubation time: 20 min. Results are expressed as mean  $\pm$  standard deviation of three independent experiments.

cells (Figure S21). Then, the subcellular distribution of RA-Resa was examined in live OSCC cells. The colocalization of signal from probe and organelle markers indicated that the probe could distribute across the whole cell, mainly in the cytoplasm rather than in specific organelles (Figure S22). To demonstrate the capability of RA-Resa to detect intracellular NADH, live cells were incubated with glucose at different concentrations prior to treatment with probe. This is because intracellular NADH levels greatly depend on the glycolysis process, which is affected by the glucose concentration. As expected, when treated with 1 mM glucose, RA-Resa stained cells showed slightly stronger fluorescence signal in yellow than in the absence of glucose (Figures 5 and S23). Meanwhile, further enhanced fluorescence was observed after incubation with a higher concentration of glucose (20 mM). This result is therefore consistent with

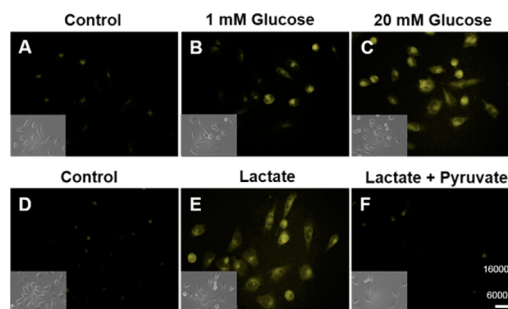


**Figure 5.** Microscopic images of probe RA-Resa (5  $\mu\text{M}$ , 15 min)-stained live OSCC cells after incubation in following conditions. (A,D) No glucose for 30 min; (B) 1 mM glucose for 30 min; (C) 20 mM glucose for 30 min; (E) 10 mM lactate for 10 min; (F) 10 mM lactate and 5 mM pyruvate for 10 min. Scale bar: 50  $\mu\text{m}$ .

previously reported work.<sup>24</sup> Meanwhile, a negligible fluorescent signal was observed in live OCSS cells after incubation with control probe **Con-Resa** (Figure S24). In addition, it was reported that the interconversion between lactate and pyruvate affects the balance of intracellular NADH and NAD<sup>+</sup> species.<sup>26</sup> As shown in Figure SE,F, strong fluorescence signal of the cells was observed after incubation with 10 mM lactate, while the cells treated with pyruvate and lactate simultaneously displayed much weaker fluorescence, indicating the roles of lactate and pyruvate in changing intracellular NADH levels. Additionally, similar phenomena were also observed in human cervical cancer cell line and Chinese hamster ovary cell lines (Figures S25 and S26). Furthermore, the NADH levels under the above conditions were quantified by NADH assay kit, which is consistent with microscopic images (Figure S27).

In conclusion, inspired by the enzyme-catalyzed sensing process, we present a novel combination-reaction two-step sensing strategy to develop fluorescent probes. Based on this bio-inspired strategy, the representative complex biomolecule, NADH, was successfully detected by the boronic acid-containing fluorescent probe, **BA-Resa**. This probe showed excellent sensitivity (detection limit: 0.084  $\mu$ M) and selectivity to NADH in alkaline conditions in the absence of any enzymes. Subsequently, this NADH probe was further modified to give **RA-Resa**, which selectively responds to NADH at intracellular concentrations at physiological pH (7.4). Significantly, the probe **RA-Resa** not only provides a simple way to detect NADH *in vitro* but also displays the feasibility to evaluate NADH levels in live cell imaging. Although there are still some drawbacks to this probe, such as photostability and ease of washout, this work provides a novel and practical approach to increase sensitivity and selectivity when designing fluorescent probes for sensing complicated biomolecules.

## ■ ASSOCIATED CONTENT

### Supporting Information

The Supporting Information is available free of charge on the ACS Publications website at DOI: 10.1021/jacs.6b05810.

Experimental details and data (PDF)

## ■ AUTHOR INFORMATION

### Corresponding Author

\*chmcyt@nus.edu.sg

### Notes

The authors declare no competing financial interest.

## ■ ACKNOWLEDGMENTS

This research was supported by an intramural funding from the A\*STAR Biomedical Research Council and Singapore Ministry of Education Academic Research Fund Tier 1 (R-143-000-602-112). We thank SBIC-Nikon Imaging Centre for confocal microscopy facilities.

## ■ REFERENCES

- (1) Zhang, J.; Campbell, R. E.; Ting, A. Y.; Tsien, R. Y. *Nat. Rev. Mol. Cell Biol.* **2002**, *3*, 906.
- (2) Stephens, D. J.; Allan, V. J. *Science* **2003**, *300*, 82.
- (3) Ntziachristos, V. *Nat. Methods* **2010**, *7*, 603.
- (4) Aron, A. T.; Ramos-Torres, K. M.; Cotruvo, J. A., Jr.; Chang, C. J. *Acc. Chem. Res.* **2015**, *48*, 2434.
- (5) Asanuma, D.; Kobayashi, H.; Nagano, T.; Urano, Y. *Methods Mol. Biol.* **2009**, *574*, 47.

- (6) Kubota, R.; Hamachi, I. *Chem. Soc. Rev.* **2015**, *44*, 4454.
- (7) Yuan, L.; Lin, W.; Zheng, K.; He, L.; Huang, W. *Chem. Soc. Rev.* **2013**, *42*, 622.
- (8) Li, H.; Fan, J.; Peng, X. *Chem. Soc. Rev.* **2013**, *42*, 7943.
- (9) Tang, Y.; Lee, D.; Wang, J.; Li, G.; Yu, J.; Lin, W.; Yoon, J. *Chem. Soc. Rev.* **2015**, *44*, 5003.
- (10) Kobayashi, H.; Ogawa, M.; Alford, R.; Choyke, P. L.; Urano, Y. *Chem. Rev.* **2010**, *110*, 2620.
- (11) Izumi, S.; Urano, Y.; Hanaoka, K.; Terai, T.; Nagano, T. *J. Am. Chem. Soc.* **2009**, *131*, 10189.
- (12) Collins, Y.; Chouchani, E. T.; James, A. M.; Menger, K. E.; Cocheme, H. M.; Murphy, M. P. *J. Cell Sci.* **2012**, *125*, 801.
- (13) Mailloux, R. J.; Lemire, J.; Appanna, V. D. *Antonie van Leeuwenhoek* **2011**, *99*, 433.
- (14) Eto, K.; Tsubamoto, Y.; Terauchi, Y.; Sugiyama, T.; Kishimoto, T.; Takahashi, N.; Yamauchi, N.; Kubota, N.; Murayama, S.; Aizawa, T.; Akanuma, Y.; Aizawa, S.; Kasai, H.; Yazaki, Y.; Kadowaki, T. *Science* **1999**, *283*, 981.
- (15) Mayevsky, A.; Rogatsky, G. G. *Am. J. Physiol. Cell Physiol.* **2007**, *292*, C615.
- (16) Ying, W. *Front. Biosci., Landmark Ed.* **2006**, *11*, 3129.
- (17) Alberghina, L.; Gaglio, D. *Cell Death Dis.* **2014**, *5*, e1561.
- (18) McNeil, C. J.; Spoons, J. A.; Cocco, D.; Cooper, J. M.; Bannister, J. V. *Anal. Chem.* **1989**, *61*, 25.
- (19) Ritov, V. B.; Menshikova, E. V.; Kelley, D. E. *Anal. Biochem.* **2004**, *333*, 27.
- (20) Xie, W.; Xu, A.; Yeung, E. S. *Anal. Chem.* **2009**, *81*, 1280.
- (21) Uppal, A.; Ghosh, N.; Datta, A.; Gupta, P. K. *Biotechnol. Appl. Biochem.* **2005**, *41*, 43.
- (22) Patterson, G. H.; Knobel, S. M.; Arkhammar, P.; Thastrup, O.; Piston, D. W. *Proc. Natl. Acad. Sci. U. S. A.* **2000**, *97*, 5203.
- (23) Freeman, R.; Gill, R.; Shweky, I.; Kotler, M.; Banin, U.; Willner, I. *Angew. Chem., Int. Ed.* **2009**, *48*, 309.
- (24) Zhao, Y.; Jin, J.; Hu, Q.; Zhou, H. M.; Yi, J.; Yu, Z.; Xu, L.; Wang, X.; Yang, Y.; Loscalzo, J. *Cell Metab.* **2011**, *14*, 555.
- (25) Zhang, L.; Li, Y.; Li, D. W.; Jing, C.; Chen, X.; Lv, M.; Huang, Q.; Long, Y. T.; Willner, I. *Angew. Chem., Int. Ed.* **2011**, *50*, 6789.
- (26) Hung, Y. P.; Albeck, J. G.; Tantama, M.; Yellen, G. *Cell Metab.* **2011**, *14*, 545.
- (27) Tu, C.; Nagao, R.; Louie, A. Y. *Angew. Chem., Int. Ed.* **2009**, *48*, 6547.
- (28) Ito, H.; Terai, T.; Hanaoka, K.; Ueno, T.; Komatsu, T.; Nagano, T.; Urano, Y. *Chem. Commun.* **2015**, *51*, 8319.
- (29) Roeschlaub, C. A.; Maidwell, N. L.; Reza Rezai, M.; Sammes, P. G. *Chem. Commun.* **1999**, 1637.
- (30) Jung, S. O.; Ahn, J. Y.; Kim, S.; Yi, S.; Kim, M. H.; Jang, H. H.; Seo, S. H.; Eom, M. S.; Kim, S. K.; Ryu, D. H.; Chang, S.-K.; Han, M. S. *Tetrahedron Lett.* **2010**, *51*, 3775.
- (31) Fomin, M. A.; Dmitriev, R. I.; Jenkins, J.; Papkovsky, D. B.; Heindl, D.; König, B. *ACS Sensors* **2016**, *1*, 702.
- (32) Slater, T. F.; Sawyer, B. *Nature* **1962**, *193*, 454.
- (33) Tsukiji, S.; Miyagawa, M.; Takaoka, Y.; Tamura, T.; Hamachi, I. *Nat. Chem. Biol.* **2009**, *5*, 341.
- (34) O'Brien, J.; Wilson, I.; Orton, T.; Pognan, F. *Eur. J. Biochem.* **2000**, *267*, 5421.
- (35) Wu, X.; Li, Z.; Chen, X. X.; Fossey, J. S.; James, T. D.; Jiang, Y. B. *Chem. Soc. Rev.* **2013**, *42*, 8032.
- (36) Wang, L.; Yuan, L.; Zeng, X.; Peng, J.; Ni, Y.; Er, J. C.; Xu, W.; Agrawalla, B. K.; Su, D.; Kim, B.; Chang, Y. T. *Angew. Chem., Int. Ed.* **2016**, *55*, 1773.
- (37) Guilbault, G. G.; Kramer, D. N.; Goldberg, P. J. *Phys. Chem.* **1965**, *69*, 3696.
- (38) Iannazzo, L.; Benedetti, E.; Catala, M.; Etheve-Quellejeu, M.; Tisne, C.; Micouin, L. *Org. Biomol. Chem.* **2015**, *13*, 8817.